



Title	Role of Surface Tension in Fusion Welding (Part 1) : Hydrostatic Effect
Author(s)	Matsunawa, Akira; Ohji, Takayoshi
Citation	Transactions of JWRI. 1982, 11(2), p. 145-154
Version Type	VoR
URL	https://doi.org/10.18910/5800
rights	
Note	

The University of Osaka Institutional Knowledge Archive : OUKA

<https://ir.library.osaka-u.ac.jp/>

The University of Osaka

Role of Surface Tension in Fusion Welding (Part 1)[†]

— Hydrostatic Effect —

Akira MATSUNAWA* and Takayoshi OHJI**

Abstract

Due to the high values of surface tension and capillary constant of liquid metal, the surface tension plays an important role in fusion welding both in static and dynamic manner. In this paper are reviewed the basic concepts of surface tension, particularly the thermodynamic derivation of capillary pressure, and mathematical approach to determine the surface profile of liquid pool from hydrostatic view point and its applicability to actual weld beads.

KEY WORDS: (Surface Tension), (Capillary Pressure), (Liquid Metal), (Welding), (Surface Profile)

1. Introduction

In fusion welding, it is well known that various kind of forces affect the welding phenomena. Such forces are the electromagnetic force, surface or interfacial tension, gravitational force, mechanical forces, and they govern the welding phenomena, in the single or combined manner, such as metal transfer, molten pool behaviors, arc characteristics and so on. The electromagnetic force is by far the most important factor among them. But, due to the high value of surface tension of liquid metal and also the small size of molten zone, the surface tension often plays very important role during welding. One can frequently observe the welding phenomena associated by the surface tension in either of static and dynamic state. Good examples of its effect are the stable suspension of molten pool without any backing system in full penetration welding of thin plate, or the smooth metal transfer of filler wire (cold wire) at the overhead position welding when the molten tip touches on the liquid pool. In both cases, the surface tension is obviously the predominant factor of governing the phenomena in the gravitational field. Many researchers have considered the effect of surface tension in individual welding phenomenon, but the systematic description of its effect in fusion welding has not been found in literatures. It is, therefore, the purpose of this series articles to review the role of surface tension in fusion welding, particularly in arc welding, from the static and dynamic fluid mechanical view point.

2. Fundamentals

2.1 Definition of surface tension

The interfacial region or simply interface is defined as the boundary between continuous bulk phases of matter¹⁾⁻³⁾. In another word, it is characterized by the thin layer of a few molecules thickness which separates two bulk phases of matter and the physical properties within this layer differ considerably from those in either of the bulk phases. Namely, there exists the surplus energy at the interface and it is called the surface free energy F^Σ , which is defined as

$$F^\Sigma = F - (F_1 + F_2) \quad (1)$$

where, F : Total free energy of two phase system including interface

F_1, F_2 : Free energy of each bulk phase.

In case of the one-component systems, the surface free energy F^Σ is a thermodynamic potential that includes two independent variables, i.e., temperature T and surface area Σ . Therefore, the following relation is derived.

$$\begin{aligned} dF^\Sigma &= \left(\frac{\partial F^\Sigma}{\partial T}\right)_\Sigma dT + \left(\frac{\partial F^\Sigma}{\partial \Sigma}\right)_T d\Sigma \\ &= -S^\Sigma dT + \sigma d\Sigma \end{aligned} \quad (2),$$

where, S^Σ : Surface entropy.

Here, the quantity

$$\sigma = \left(\frac{\partial F^\Sigma}{\partial \Sigma}\right)_T \quad (3)$$

is the surface free energy per unit area at constant temperature. It is obvious that the work of reversible isothermal expansion of the surface, dW , is equal to

[†] Received on September 30, 1982

* Associate Professor

** Associate Professor, Department of Welding Engineering, Faculty of Engineering, Osaka University

Transactions of JWRI is published by Welding Research Institute of Osaka University, Ibaraki, Osaka, Japan

the decrease in free energy, i.e.,

$$dW = -\sigma d\Sigma \tag{4}$$

and hence the quantity σ is usually called interfacial tension or surface tension and has the unit of (dyne/cm) or (erg/cm²) in C.G.S. unit or (N/m) or (J/m²) in S.I. unit.

2.2. Equilibrium conditions between two phases at rest and capillary pressure²⁾

Necessary conditions of thermodynamic equilibrium²⁾ are

- 1) Equal temperature in both phases, and
- 2) The minimum state of the free energy of the system, i.e., $\delta F = 0$.

Now, let us consider two bulk phase 1 and 2 at rest separated by the surface element $d\Sigma$. The equilibrium condition of this system is

$$\delta F = \delta F_1 + \delta F_2 + \delta F^\Sigma = 0 \tag{5}$$

The change in free energy of the system at constant temperature can only occur as the result of changes in the volume of two phases and area of interface. Namely,

$$\delta F_1 = -p_1 \delta V_1 \tag{6}$$

$$\delta F_2 = -p_2 \delta V_2 \tag{7}$$

$$\delta F^\Sigma = \sigma \delta \Sigma \tag{8}$$

Under the condition of constant total volume,

$$\delta V_1 = -\delta V_2.$$

Therefore, the total change in the free energy of the system is

$$\delta F = -(p_1 - p_2) \delta V_1 + \sigma \delta \Sigma \tag{9}$$

Here, let us suppose that the surface element $d\Sigma_0 (= dx dy)$ on a flat interface is displaced arbitrarily and infinitesimally along the normal to the undeformed surface ($z=0$). (See Fig.1.) Let us also assume that the displacement occurs in the plane $y = \text{const.}$, producing a surface that is curved in only one direction. The change in area is then

$$\begin{aligned} d\Sigma &= \sqrt{1 + \left(\frac{\partial \zeta}{\partial x}\right)^2} d\Sigma_0 \\ &= \sqrt{1 + \left(\frac{\partial \zeta}{\partial x}\right)^2} dx dy \end{aligned} \tag{10}$$

where ζ is the vertical displacement over the plane $z = 0$. At small displacement ζ , the equation (10) is approximated by

$$d\Sigma \approx \left\{ 1 + \frac{1}{2} \left(\frac{\partial \zeta}{\partial x}\right)^2 \right\} dx dy.$$

The surface area after deformation is thus obtained as

$$\Sigma = \iint \left[1 + \frac{1}{2} \left(\frac{\partial \zeta}{\partial x}\right)^2 \right] dx dy.$$

Now, back to the equations (8) and (9), the change in the surface area $\delta \Sigma$ is

$$\begin{aligned} \delta \Sigma &= \iint \frac{\partial \zeta}{\partial x} \frac{\partial \delta \zeta}{\partial x} dx dy \\ &= \int \left(\frac{\partial \zeta}{\partial x} \delta \zeta \Big|_a^b \right) dy - \iint \frac{\partial^2 \zeta}{\partial x^2} \delta \zeta dx dy \\ &= - \iint \frac{\partial^2 \zeta}{\partial x^2} \delta \zeta dx dy \end{aligned} \tag{11}$$

since two surface points may be considered fixed, i.e., $\delta \zeta_a = \delta \zeta_b = 0$.

The variation in volume δV_1 of the first phase made by an infinitesimal displacement of points on the surface is

$$\delta V_1 = \iint \delta \zeta dx dy \tag{12}$$

Substituting equations (11) and (12) into the equation (9),

$$\delta F = \iint \left[-(p_1 - p_2) - \sigma \frac{\partial^2 \zeta}{\partial x^2} \right] \delta \zeta dx dy \tag{13}$$

In an equilibrium state, the free energy must be minimum, i.e., $\delta F = 0$. Since $\delta \zeta$ is an arbitrary and infinitesimal quantity, it follows from the equation (13) that

$$p_\sigma \equiv p_1 - p_2 = -\sigma \frac{\partial^2 \zeta}{\partial x^2} \tag{14}$$

The most important physical meaning of the relation (14) is that the pressure difference between two phases is always associated by the surface tension

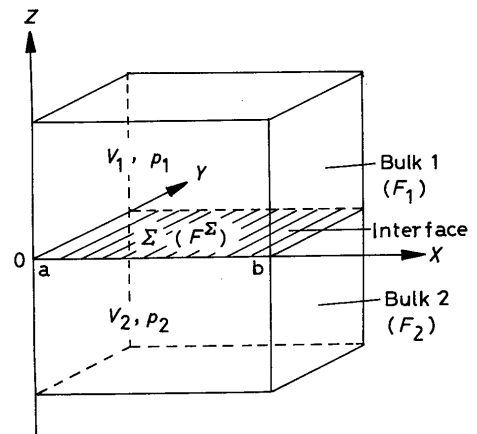


Fig. 1 Two bulk phases separated by interface

unless the interface is a flat plane. This pressure difference is called **Capillary Pressure** and always acts normal to the surface on it.

The above is the discussion when the surface is infinitesimally distorted from the flat plane along x -direction. In more general case that the interface is initially curved finitely along x -direction, the capillary pressure is expressed as

$$P_\sigma = -\sigma \frac{\left(\frac{d^2\zeta}{dx^2}\right)}{\left\{1 + \left(\frac{d\zeta}{dx}\right)^2\right\}^{3/2}} \quad (15).$$

Another expression of capillary pressure in three dimensional surface is usually written in the form of

$$p_\sigma = \sigma \left(\frac{1}{R_1} + \frac{1}{R_2}\right) \quad (16),$$

where R_1 and R_2 are the principal radii of curvature of the surface. This equivalent equation to (15) is well known as **Laplace's Equation of Pressure**, which is easily derived from the force balance of a stretched film having the curvature R_1 and R_2 in x - and y -directions³⁾.

2.3. Rise of liquid in a circular capillary and definition of capillary constant

The most famous phenomenon associated by capillary pressure is the rise of liquid in a capillary. Let us suppose a fine tube placed vertically on the liquid (**Fig. 2**) and consider the pressure balance at the plane $z = 0$.

$$p_0 - p_\sigma + \rho gh = p_0 \quad (17)$$

If the radius of capillary is very small, the meniscus curvatures R_1 and R_2 inside the capillary are approximated by $R_1 = R_2 \approx r$ and the equation (16) becomes

$$p_\sigma = \frac{2\sigma}{r} \quad (18).$$

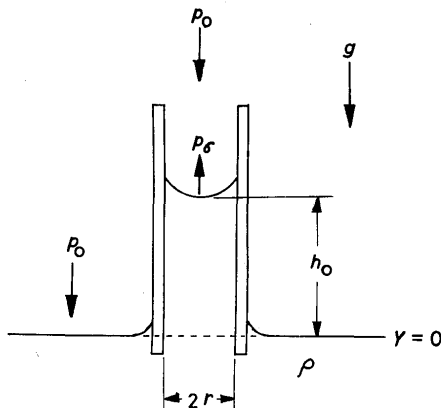


Fig. 2 Pressure balance in circular capillary

Therefore, the capillary rise h_0 is readily given from the equation (17) as

$$h_0 = \frac{1}{r} \frac{2\sigma}{\rho g} \quad (19a).$$

It is obvious from the equation (19a) that the quantity $\sqrt{2\sigma/(\rho g)}$ has the dimension of length. $\sqrt{2\sigma/(\rho g)}$ is generally called **Capillary Constant** and it is one of the measure or criterion if one should take into account the effect of surface tension or not in the considering system. Namely, if the characteristic size of liquid is comparable to or smaller than the capillary constant, one has to always consider the capillary effect.

The capillary constant is also an important parameter to express the related equations in non-dimensional forms. Denoting the constant as

$$h^* \equiv \sqrt{\frac{2\sigma}{\rho g}} \quad (20),$$

then the equation (19a) is expressed by a dimensionless form as

$$\frac{h_0}{h^*} = \frac{1}{(r/h^*)}$$

or

$$H_0 = 1/A \quad (19b)$$

where, $H_0 = h_0/h^*$ and $A = r/h^*$ are the dimensionless height and radius respectively.

2.4. Surface tension of liquid metal⁴⁾

In **Table 1** are shown some example of surface tension and capillary constant of liquid elements at the vicinity of their melting points. The elements that are related to welding material have very high surface tension compared with mercury which is often sited as the high surface tension material. In general, the surface tension is higher in higher melting point material as shown in **Fig. 3**, but there exists no simple relation between them⁴⁾. An interesting feature of surface tension is that its value changes periodically with the atomic number⁴⁾ as seen in **Fig. 4**, which suggests that the tension is closely related to the valency electrons state of element.

As described in previous section 2.1., the surface tension of one-component system is the function of temperature T and surface area Σ . The temperature coefficient of surface tension of all one-component liquids is always negative, i.e., $(\partial\sigma/\partial T) < 0$. Namely, the surface tension decreases with the increase of temperature.

Table 1 Surface tension and capillary constant of several liquid elements

Element	Ambient	Melting Point (°C)	Temperature (°C)	Surface Tension (dyne/cm)	Capillary Const. (cm)
H ₂ O	Air	0	25	71.97	0.383
Hg	Vac.	-38.9	25	484	0.269
Sn	Vac.	232	250	≈550	≈0.400
Pb	Vac.	327	330	≈450	≈0.293
Zn		419	420	773	0.490
Al	Vac.	660	800	≈850	≈0.854
Ag	H ₂	961	1000	≈1000	≈0.477
Cu	Vac.	1083	1083	1300	0.576
Ni	Vac.	1455	1455	≈1700	≈0.668
Fe	Vac.	1535	1535	1500 - 1800	0.661 - 0.724
Mo	Vac.	2620	2620	2080	0.674
W	Vac.	3410	3410	2300 - 2500	0.518 - 0.540

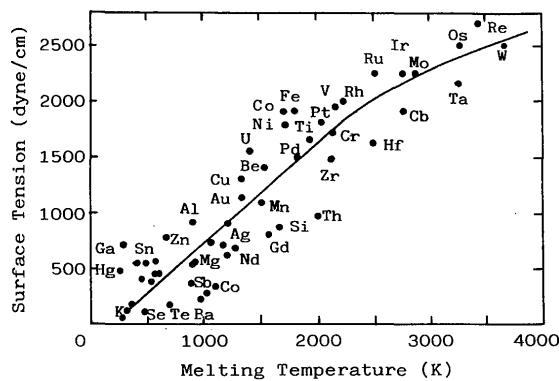


Fig. 3 Surface tension of liquid metal at their melting points versus melting temperature⁴⁾

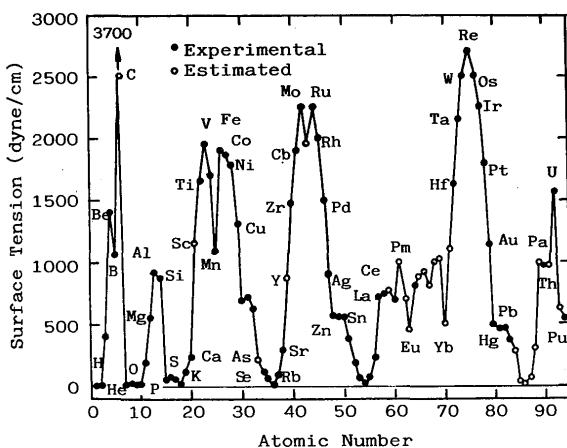


Fig. 4 Surface tension of liquid elements at their melting points versus atomic number⁴⁾

The effect of impurities on surface tension is important for actual welding. In Figs. 5, 6 & 7 are shown same examples of the soluble materials effects in base elements⁴⁾. Almost all the alloying elements reduce the surface tension, particularly the effect of oxygen, sulfur, selenium, antimony and tin are drastic even at the very small addition. It is interesting to

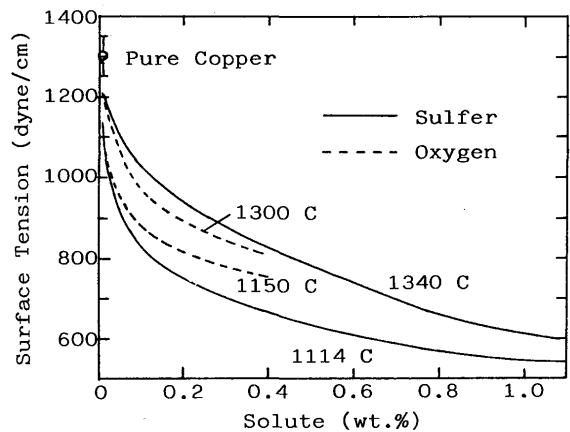


Fig. 5 Effect of Sulfur, Oxygen and temperature on surface tension of Copper⁴⁾

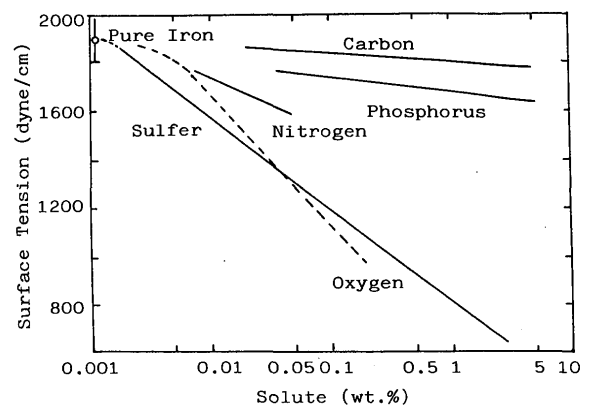


Fig. 6 Effect of nonmetallic elements on surface tension of liquid Iron at 1550 - 1570°C⁴⁾

compare with Fig. 4, that these elements belong to the group showing the very small value under the condition of pure element.

The effect of temperature on surface tension in actual alloys is not clear. Many alloys show the negative characteristic like as pure element, while

there are some materials which have the positive temperature coefficient as seen in the Fig. 5.

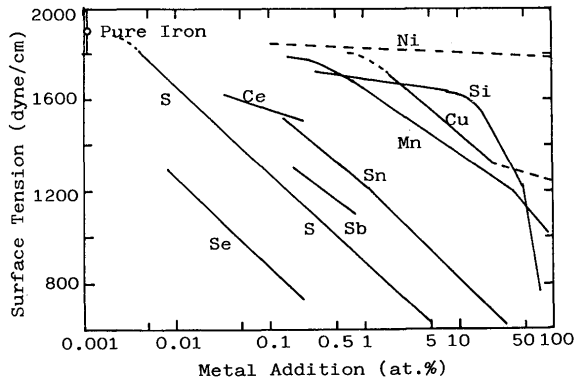


Fig. 7 Effect of binary metal additions on surface tension of liquid Iron at 1550 – 1570°C⁴

3. Surface Profile of Liquid and Weld Beads^{5~10}

3.1. Static pressure balance of two-dimensional liquid pool and bead surface shape in flat position

Mathematical calculation of liquid meniscus in a capillary was conducted by many researchers. Since the equation of meniscus of axisymmetry can not be solved analytically, the calculation must be done by numerical methods. Very precise calculations in higher order approximation were carried by Poisson (1831), Rayleigh⁵ (1915) for small diameter capillary, and Bashforth and Adams⁶ (1883) for larger diameter. For the liquid placed on the flat plate, the profile was numerically calculated by Bashforth and Adams⁶ (1883) and Ferguson⁷ (1913), and the results are widely used to measure the surface tension by sessile drop method. Prandtl and Tietjens⁸ (1934) described in their book that the meniscus of two dimensional liquid was expressed by the elliptic integral, and Nishiguchi and Ohji^{9~15} (1976) conducted the calculation for applying to the weld pool. They also developed a numerical analysis of three dimensional pool in 1978^{9,15}. Here will be only described the two dimensional analysis of liquid pool and its application to welding bead.

Let us suppose a two-dimensional liquid pool as shown in Fig. 8, assuming that the surface tension is constant over the surface. The static pressure balance at point P(x,y) is

$$\frac{\sigma}{R} = \frac{\sigma}{R_0} - \rho gy \quad (21),$$

where, $1/R_0$: Curvature at origin
 $1/R$: Curvature at point P

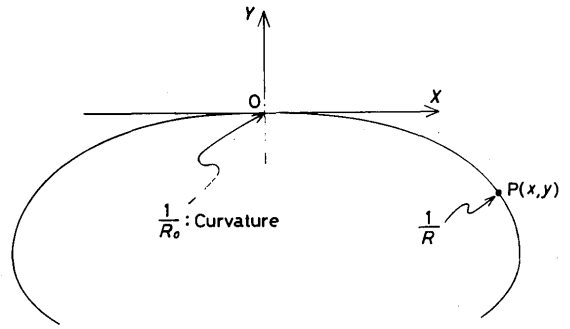


Fig. 8 Two-dimensional liquid pool placed horizontally⁹

- σ : Surface tension
- ρ : Density of liquid
- g : Acceleration of gravity.

From the equivalence of equations (15) and (16), R is written in the form of

$$\frac{1}{R} = \pm \frac{d^2y/dx^2}{(1 + (dy/dx)^2)^{3/2}} \quad (22).$$

Here, R is taken positive when the origin stays in liquid side and vice versa.

Combining equations (21) and (22), and integrating with respect to y ,

$$-\frac{1}{(1 + (dy/dx)^2)^{1/2}} = \frac{\rho g}{2\sigma} y^2 - \frac{1}{R_0} y + C \quad (23).$$

At the origin ($x=y=0$), $dy/dx = 0$, therefore $C = -1$.

$$-\frac{1}{(1 + (dy/dx)^2)^{1/2}} = \frac{\rho g}{2\sigma} y^2 - \frac{1}{R_0} y - 1 \equiv f(y) \quad (24)$$

$$-1 \leq f(y) \leq 0.$$

Once again integrating equation (24) with respect to y ,

$$x = \pm \frac{1}{2} \int_0^y \left[\frac{\sqrt{1+f(y)}}{\sqrt{1-f(y)}} - \frac{\sqrt{1-f(y)}}{\sqrt{1+f(y)}} \right] dy \quad (25).$$

Since the function $f(y)$ is a quadratic equation, the right side of equation (25) has the form of elliptic integral. Therefore, the equation (25) is expressed as

$$x = \pm \frac{1}{\sqrt{a(1+b)}} \left\{ (1+b) \left[E(\psi, s) - E\left(\frac{\pi}{2}, s\right) \right] - b \left[F(\psi, s) - F\left(\frac{\pi}{2}, s\right) \right] \right\} \quad (26a)$$

$$\cos \psi = \sqrt{a(y^2 - 2ky)/2} \quad (26b)$$

- where, $E(\psi, s)$: Elliptic integral of the 2nd kind
- $F(\psi, s)$: Elliptic integral of the 1st kind
- $a = \rho g / (2\sigma)$: Constant ($a = 1/h^*$)
- $b = 1 + (\sigma / (2\rho g R_0^2))$
- $k = \sigma / (\rho g R_0)$
- $s = (2/(1+b))^{1/2}$

Thus, the surface profile of two-dimensional liquid placed on a flat place can be calculated from equations (24) and (26).

For example, the height of liquid that has the contact angle of $\theta = \pi/2$ on a plate is obtained from the equation (24) putting $dy/dx = -\infty$.

$$h_{\theta=\pi/2} = \frac{\sigma}{\rho g R_0} \left\{ \sqrt{1 + \frac{2\rho g R_0^2}{\sigma}} - 1 \right\} \quad (27).$$

The width of liquid W_B on a plate having the above height is calculated from the equation (26) as

$$W_{B\theta=\pi/2} = \frac{2}{\sqrt{a(1+b)}} \left\{ (1+b) \left[E\left(\frac{\pi}{4}, s\right) - E\left(\frac{\pi}{2}, s\right) \right] - b \left[F\left(\frac{\pi}{4}, s\right) - F\left(\frac{\pi}{2}, s\right) \right] \right\} \quad (28).$$

Figure 9 shows the relation between height and width calculated from equations (27) and (28). The maximum height at very large width is the same with the capillary constant for $\theta = \pi/2$, which is readily obtained from equation (27) under the condition of $R_0 = \infty$.

The volume of liquid is a particular interest in case of welding, because it is related with the amount of deposit metal. Figure 10 illustrates the method of calculating the volume having an arbitrary angle on a plate. The force balance on the y_0 -plane in the vertical direction is given as follows.

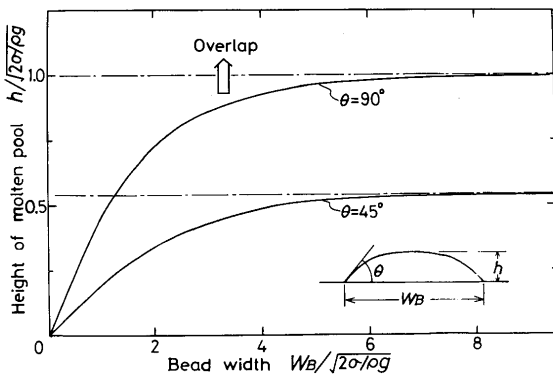


Fig. 9 Relation between width and height of liquid having constant contact angle on flat plate⁹⁾

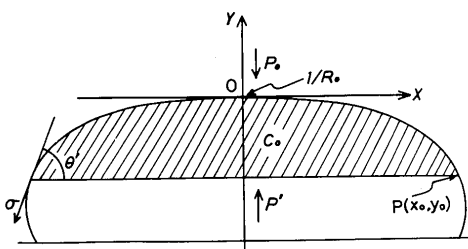


Fig. 10 Force balance on y_0 -plane⁹⁾

$$\left(\frac{\sigma}{R_0} - \rho g y_0\right) \cdot 2x_0 - 2\sigma \sin \theta = \rho g C_0 \quad (29)$$

where C_0 is the liquid volume of hatched area in Fig. 10. Eliminating R_0 from equation (29), combining with equation (24), one obtains the liquid volume that has the contact angle θ and bead width W_B .

$$C_0 = \left(h + \frac{2\sigma}{\rho g} \frac{1 - \cos \theta}{h}\right) \frac{W_B}{2} - \frac{2\sigma}{\rho g} \sin \theta \quad (30)$$

Figure 11 shows the calculated volume versus width for the angle of 90° and 45° . Here, the conditions that the angle over 90° and less than 0° are defined as overlap and undercut (or underfill) bead respectively. Figure 12 shows the calculated critical conditions of overlapping and undercutting in V-grooves of various angle.

In the following will be described the comparison of the above calculation with actual welding beads. In Figure 13 are shown the measured height and width of beads obtained in non-shielded arc and manual arc welding on a flat plate, in which the open and solid marks represent that the contact angle is less than or over 90° . The calculated line of $\theta = 90^\circ$ well fits with the experimental values. It should be noted here that the capillary constant in case of non-shielded arc

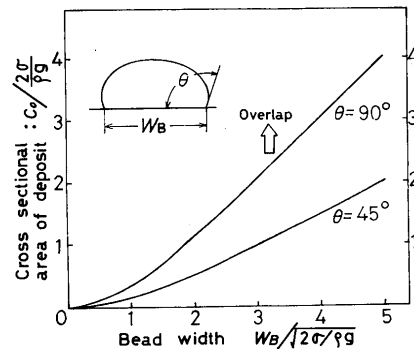


Fig. 11 Liquid volume versus bead width under the constant contact angle⁹⁾

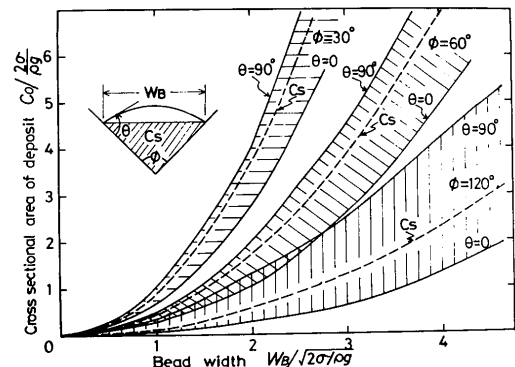


Fig. 12 Liquid volume versus bead width in V-grooves⁹⁾

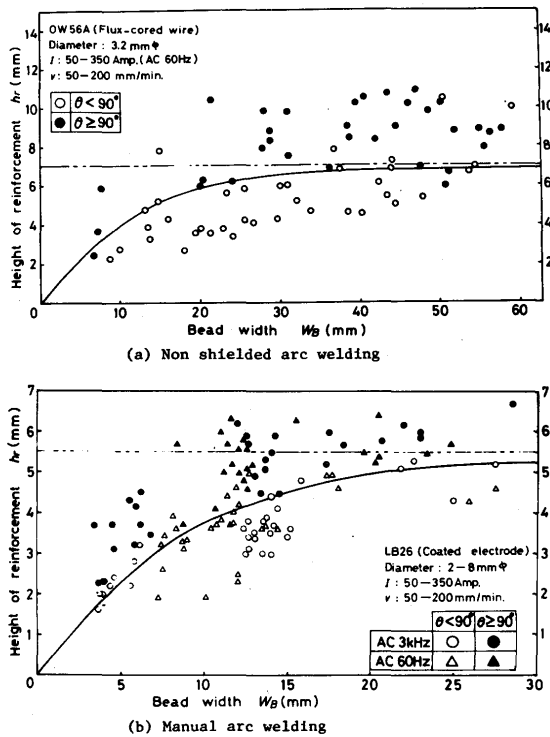


Fig. 13 Calculated and measured height of reinforcement of welded metal on flat plate⁹⁾

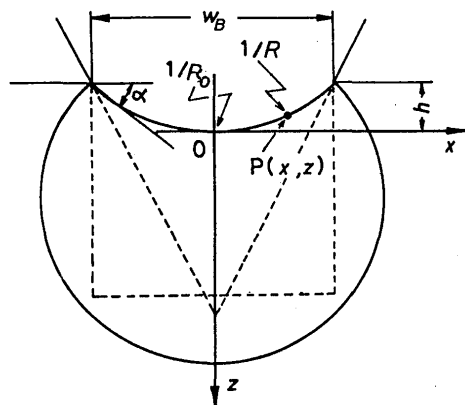


Fig. 14 Pressure balance of liquid surface in narrow V- and I-grooves¹⁶⁾

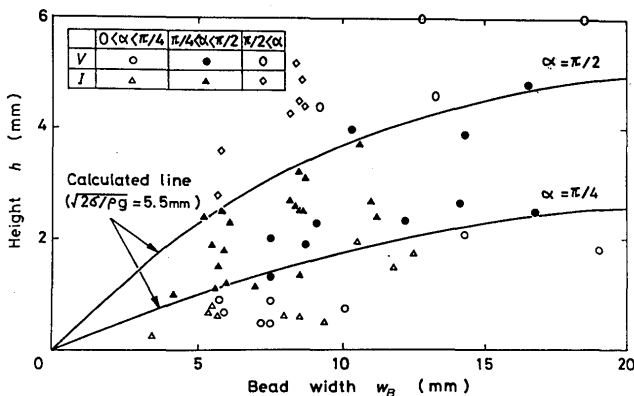


Fig. 15 Calculated and measured bead profile in narrow gap MIG welding¹⁶⁾

welding is 7 mm which seems rather high as a conventional steel. In this process, thick molten slag covers over the molten pool, so that one has to take into account the interfacial tension and slag density. Therefore, the effective capillary constant may be expressed as $\sqrt{2\sigma/(\rho-\rho_0)g}$ instead of the definition given in equation (20).

The calculation is also applicable for the dented pool in a groove as shown in Fig. 14, if the curvature is taken negative. Figure 15 shows the experimental values of height and width in cases of narrow V- and I-groove MIG welding, where one sees that the actual beads having the toe angle between 45° and 90° stay in the region bounded by the calculated line¹⁶⁾.

In Figures 16 and 17 are compared the calculated cross sectional area of deposit metal with experimental values in overlay welding by the non-shielded and strip electrode submerged arc processes. Here again one sees fairly good coincidence.

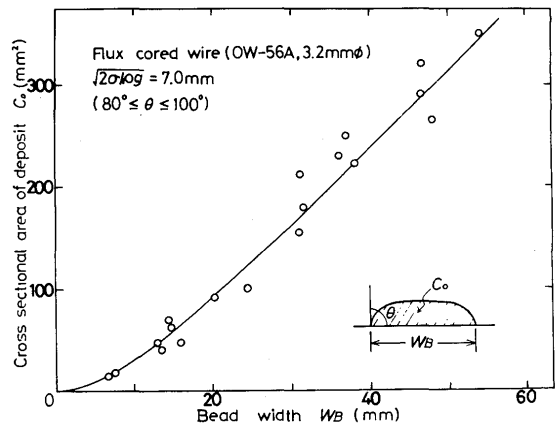


Fig. 16 Cross sectional area of deposit metal under the critical condition of overlapping in non-gas shielded arc welding⁹⁾

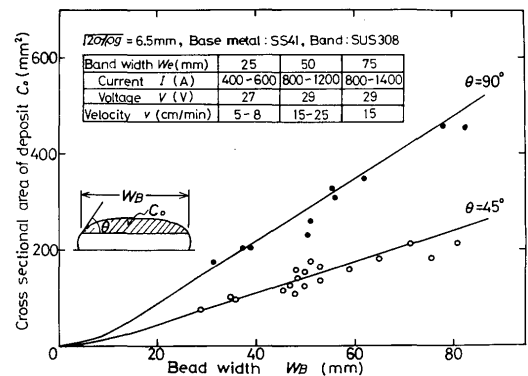


Fig. 17 Cross sectional area versus bead width in overlay welding by submerged arc with strip electrode⁹⁾

3.2. Bead surface shape of horizontal fillet welding

In this section will be described the surface profile of bead in the horizontal fillet welding. Let us suppose a two-dimensional liquid placed at the corner of the vertical and horizontal plates to which the liquid contacts at the points A and B as shown in Fig. 18. The basic equations of pressure balance are the same with the previous equations of (21) and (22). The boundary condition in this case is

$$(dy/dx) = -\cot \alpha \text{ at point A } (x = y = 0) \quad (31)$$

Putting this boundary condition into the previous equation (23), the integral constant becomes

$$C = -1/(1 + \cot^2 \alpha)^{1/2} = -\sin \alpha$$

Therefore, the surface profile under the question is given by

$$x = \frac{1}{2} \int_0^y \left[\frac{\sqrt{1+g(y)}}{\sqrt{1-g(y)}} - \frac{\sqrt{1-g(y)}}{\sqrt{1+g(y)}} \right] dy \quad (32),$$

where,

$$g(y) = \frac{\rho g}{2\sigma} y^2 - \frac{1}{R_0} y - \sin \alpha \quad (33). \\ -1 \leq g(y) \leq 0.$$

The cross sectional area can be also calculated from the above.

In connection with the actual horizontal fillet welding, the primary concern is how the bead surface profile changes with the leg lengths and amount of deposit metal. Figures 19 and 20 show the calculated results showing the effect of deposit metal and leg length on the bead shape for several leg length ratios. The normal liquid shape that has no undercutting

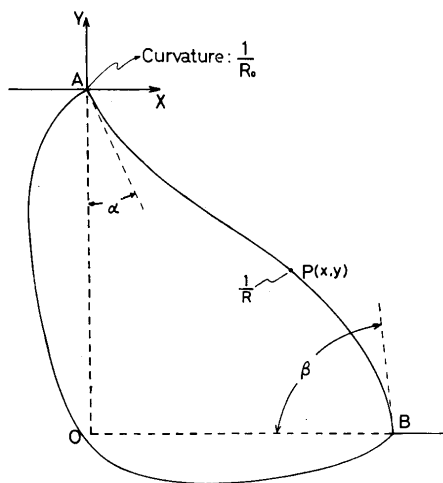


Fig. 18 Two-dimensional model of molten pool in horizontal fillet welding⁹⁾

(underfilling) nor overlapping on the vertical and horizontal plates is only expected in the hatched region (Normal Region) in the figures and the maximum leg length on horizontal plate never exceeds twice of capillary constant. Here, the definition of undercutting on the vertical plate and overlapping on the horizontal plane are $\alpha < 0$ and $\beta > 90^\circ$ respectively in Fig. 18. In the normal region, there are three types of surface profile depending on the liquid volume as seen in Fig. 21.

In Fig. 22 are compared the calculated critical conditions of undercutting and overlapping with actual beads obtained in non-gas shielded arc welding. Most of the data agree fairly well with the calculation within $\pm 10\%$ accuracy, except in very high speed welding using high current density arcs.

The above stated calculations are based on the assumptions that

- 1) The molten pool is long enough along the welding direction (Two-dimensional shape),
- 2) The liquid is still, and
- 3) Surface tension is constant over the surface.

In actual welding, however, the puddle has three dimensional shape, and there is liquid flow in the molten pool particularly at high current-high speed welding. Also, the surface tension is not always uniform over the surface. Therefore, there is naturally some limitation in applicability of the above stated calculation, but the quantitative analysis on this matter has not been established yet. Here, some unapplicable examples will be shown in Fig. 23 in case of fillet welding.

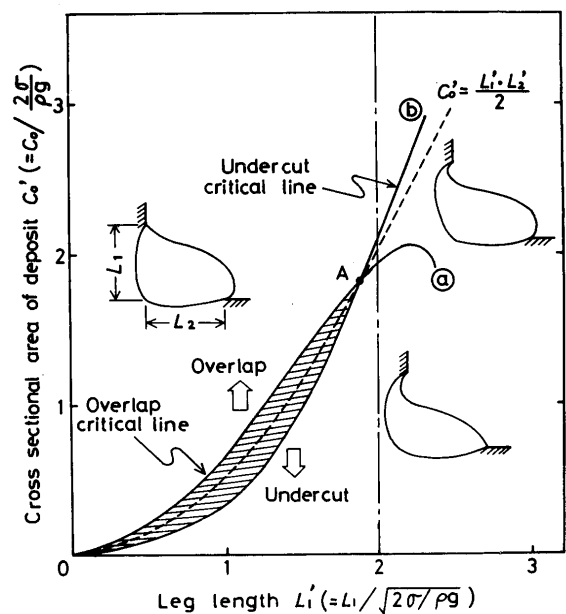


Fig. 19 Critical conditions of undercutting and overlapping in horizontal fillet welding with equi-leg-lengths⁹⁾

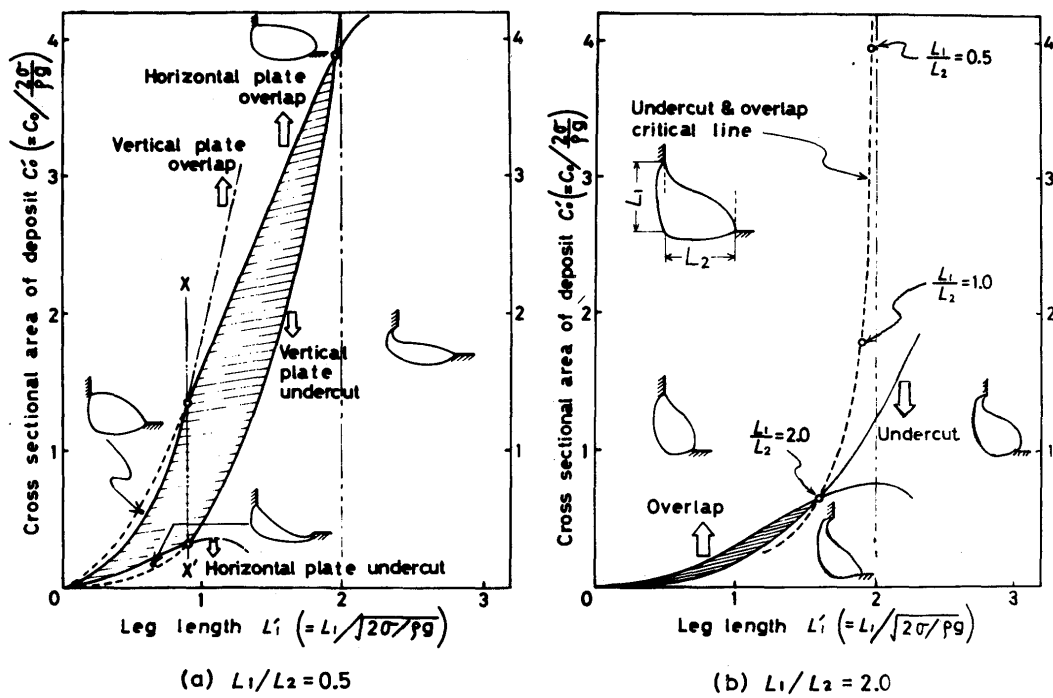


Fig. 20 Effect of leg-length ratio on critical conditions of undercutting and overlapping⁹⁾

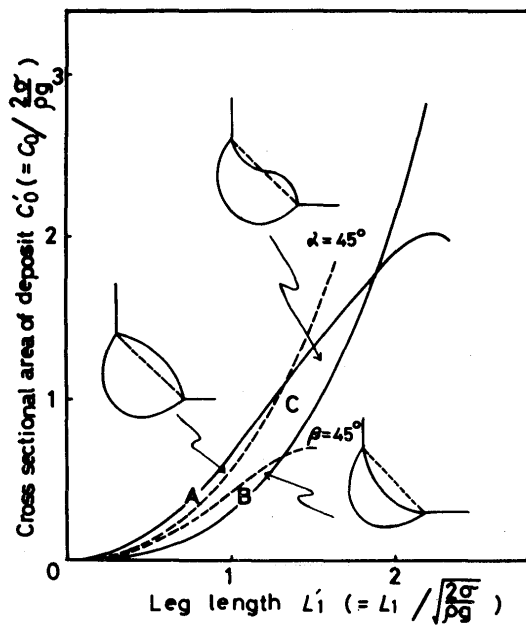


Fig. 21 Three types of surface profiles in normal fillet welding ($L_1/L_2 = 1.0$)⁹⁾

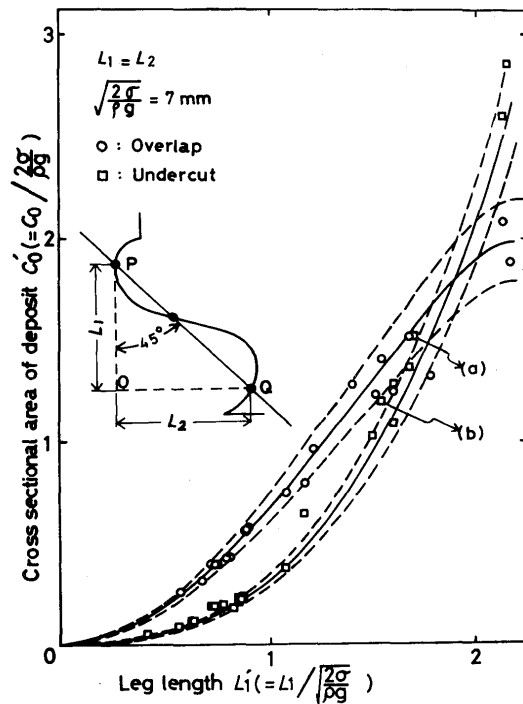


Fig. 22 Comparison of calculation with experimental values under the critical conditions of undercutting and overlapping in non-gas shielded arc process ($L_1/L_2 = 1.0$. Broken curves show the $\pm 10\%$ deviation from calculation.)⁹⁾

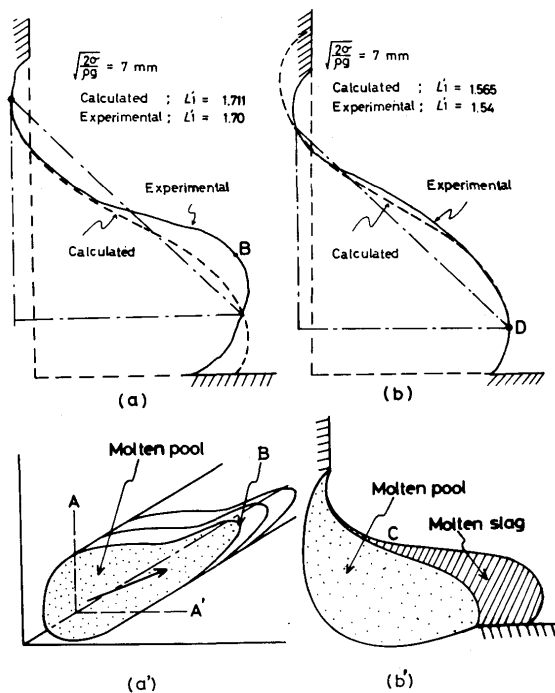


Fig. 23 Typical examples of bead profile that do not coincide with calculation⁹⁾

- (a) Existence of strong liquid flow
 (b) Uneven coverage of slag

4. Summary

In this paper were reviewed some basic concepts of surface tension and capillary pressure, mathematical analysis of two-dimensional liquid pool at rest from hydrostatic view point, and its applicability on actual welding beads. It has been shown here that the effect of surface tension is very important in weld bead shape, though the pool size (width) seems too large to consider capillarity compared with usual capillary actions observed in normal liquids such as water and so on. This is primarily due to the fact that liquid metal has very high values of surface tension itself and capillary constant. Here, the calculating method of liquid surface profile was only described for the cases of flat and horizontal fillet positions, but the basic pressure balance equation naturally hold at any position. It has been experimentally confirmed that the actual solidified bead surface shape well reflects the calculated surface profile of liquid in wide range of welding condition except the high current-high speed

welding. There are many other welding phenomena that the surface tension plays an important role. In the succeeding reports of this series will be described the self suspension of liquid and liquid motion induced by surface tension.

References

- 1) J.T. Davies and E.K. Rideal; *Interfacial Phenomena*, Academic Press, New York(1963), Chapter 1, p.1 - 55.
- 2) V.G. Levich; *Physicochemical Hydrodynamics*, Prentice-Hall, Englewood Cliffs (1962), Chapter VII, p. 372 - 394.
- 3) S. Ono; *Surface Tension*, Kyoritsu Shuppan, Tokyo (1980) (in Japanese)
- 4) S.Z. Beer; *Liquid Metals Chemistry and Physics*, Marcel Dekker, New York (1972), Chapter 4, p. 161 - 212.
- 5) L. Rayleigh; "Oh the Theory of Capillary Tube", Proc. Roy. Soc. A., 92 (1915), p. 184 - 195.
- 6) F. Bashforth and J.C. Adams; *An Attempt to Test the Theories of Capillary Action*, Cambridge Univ. Press, Cambridge (1883).
- 7) A. Ferguson; "Oh the Theoretical Shape of Large Bubbles and Drops", Phil. Mag., 25 (1913), p. 507 - 520.
- 8) L. Prandtl and O.G. Tietjens; *Fundamentals of Hydro- and Aeromechanics*, Chap. 4, Dover Publications, New York (1934).
- 9) T. Ohji; "Surface Tensional Analysis on Surface Profile of Weld Bead and Selfsustaining of Molten Pool", Thesis for Doctorate, Osaka University, 1978 (in Japanese)
- 10) K. Nishiguchi, T. Ohji, et al.; "Bead Formation Phenomena in Non-shielded Arc Welding", Journal of JWS, 44, 10 (1975), p. 848 - 854. (in Japanese)
- 11) *ibid.*; "Fundamental Studies on Overlay and Fillet Welding (Report 1)", *ibid.*, 45, 1 (1976), p. 82 - 87. (in Japanese)
- 12) *ibid.*; "ibid. (Report 2)", *ibid.*, 45, 2 (1976), p. 143 - 149. (in Japanese)
- 13) *ibid.*; "Mechanism of Bead Formation in Non Shielded Arc Welding", Proc. of 2nd International Symposium of Japan Welding Society, Osaka, 1975, No. 2-2-(25), p. 427 - 432.
- 14) *ibid.*; "Study on Bead Surface Profile", IIW Doc. 212-391-77, 1977.
- 15) *ibid.*; "Study on Behavior of Molten Pool in Arc Welding (2nd Report) - Numerical Analysis of Molten Pool Surface Profile -", Journal of JWS, 50, 5 (1981), p. 525 - 530. (in Japanese)
- 16) A. Matsunawa and K. Nishiguchi; "Arc Behaviour, Plate Melting, and Pressure Balance of the Molten Pool in Narrow Grooves", Proc. of International Conference on Arc Physics and Weld Pool Behaviour, London, May, 1979, p. 301 - 310.